Available online at www.sciencedirect.com

ScienceDirect

Procedia CIRP 108 (2022) 77–81

www.elsevier.com/locate/procedia

6th CIRP Conference on Surface Integrity

# The effect of femto-second laser shock peening on the microstructures and surface roughness of AlSi10Mg samples produced with selective laser melting (SLM).

Erica Liverani[a], Yuxin Li[b], Alessandro Ascari[a], Xin Zhao[b], Alessandro Fortunato[a]*

[a] *University of Bologna, Viale Risorgimento 2, 40136 Bologna, Italy*

* Corresponding author. Tel.: +39 051 2093456; *E-mail address:* alessandro.fortunato@unibo.it

**Abstract**

Post processing operations in selective laser melting (SLM) are becoming increasingly important to be able to have components with maximum performance. With this paper, the authors present the first results relating to microstructural modifications obtained after a femtosecond laser shock peening treatment (f-LSP) with a pulse duration of 165 fs and energy per pulse varying between 200-600 μJ. The samples produced with SLM were obtained by varying both the energy and scanning parameters and the surfaces treated with f-LSP are both parallel and orthogonal to the build direction.



*Keywords:* Selective Laser Melting, femto-second laser shock peening, AlSi10Mg

## 1. Introduction

Laser shock peening (LSP) is a surface engineering technique that increases material characteristics such as surface hardness, fatigue life, and corrosion resistance by promoting negative residual stresses in the material [1–5], also in aluminum alloys. When a high-intensity laser beam impacts a sample surface, the expansion of laser-induced plasma near the surface generates a severe shock wave into the sample. A nanosecond laser is generally utilized in current laser shock peening technology, which is commercially used in the automotive, aerospace, nuclear, and medical fields. Due to insufficient shock wave intensity and significant surface thermal damage, nanosecond laser shock peening (ns-LSP) requires a confined medium (e.g. water or glass) and a protective coating [8–13]. These extra procedures add to the cost and complexity of dealing with complex geometry. Femtosecond laser shock peening (fs-LSP) is a viable alternative to ns-LSP because it can generate a larger shock wave due to the ultra-high laser intensity while reducing thermal damage due to the small heat-affected zone [14]. Furthermore, the reduced plasma shielding effect improves the energy deposition efficiency due to the ultra-short laser pulse duration.

In [15] it is shown how femtosecond laser peening is affected by processing circumstances (air/water, with/without coating) and laser parameters and it was proved that an enhancement of the surface hardness by 45.5%, without any confining medium and protective coating, due to its extremely high laser-induced shock wave, can be obtained. The goal of this work is to verify which structural changes are generated on AlSi10 samples fabricated by SLM, because products created by SLM can benefit significantly from a treatment like fs-LSP, especially if they must be subjected to dynamic loads. With this paper, the authors present the first results relating to microstructural modifications obtained after a fs-LSP with a pulse duration of 165 fs and energy per pulse varying between 200-600 μJ. The


10.1016/j.procir.2022.03.017

samples produced with SLM were obtained by varying both the energy and scanning parameters and the surfaces treated with f-LSP are both parallel and orthogonal to the build direction. Initial results show that: (i) roughness has a significant impact on laser absorption and, as a result, on peening: smooth surfaces are much better treated than rough ones; and (ii) the zones where surface modifications occurred are distinguished by a resolidified area and a transition area with a refined grain.

## 2. Materials and methods

### 2.1 Sample fabrication by SLM

AlSi10Mg coupons were produced by SLM in form of blocks with a 20 x 20 mm2 square base and 3 mm in thickness. Powder was provided by Carpenter Additive (Carpenter Technology Corporation, USA) with chemical composition summarized in Table 1.

Before the process, powders were subjected to a drying pre-treatment at 60°C for 3 h and the manufacturing was carried out in a nitrogen environment with a low oxygen content (0.1 vol.%). All samples were fabricated in a SISMA MySint 100 RM metal machine with a focused spot diameter of 55 µm and were built on an aluminum platform without pre-heating.

Table 1. Chemical composition of the AlSi10 powders.

| Al | Si | Mg | Fe | Ti | Others |
|---|---|---|---|---|---|
| Balance | 9.97 | 0.38 | 0.11 | 0.01 | <0.01 |

Table 2. SLM process parameters

| | MP | | | RM | | |
|---|---|---|---|---|---|---|
| | $MP_1$ | $MP_2$ | $MP_3$ | $RM_1$ | $RM_2$ | $RM_3$ |
| Power [W] | 175 | | | | | |
| Scan speed [mm/s] | 800 | 1025 | | ≡ MP | 1000 | 800 |
| Layer thickness [µm] | 20 | 30 | | | 20 | 30 |
| Hatch spacing [µm] | 70 | 70 | | | 70 | 70 |
| Energy density [J/mm$^3$] | 137 | 71 | | | 137 | 71 |
| Scan strategy | SS1 | SS2 | SS3 | | SS1 | SS2 |

Eighteen (18) SLM setup combination were defined changing the main process parameters (MP), the building orientation (BD) and the surface remelting parameters (RM) for a total of 54 samples considering 3 repetitions of each set. In particular, the 3 main process parameters were defined following author's previous optimization [16] and literature results [17], changing the scanning strategy, as detailed in Table 2 where:

- SS1 indicates a chessboard scanning strategy with 3mm x 3mm islands rotated of 45° between subsequent layers; the skywriting is enabled
- SS2 indicates a chessboard with 2.4 mm x 2.4 islands, translated of 1 mm and rotated of 90° between subsequent layers; the skywriting is enabled
- SS3 indicated a meander scanning strategy without rotation between subsequent layers.

Regarding the influence of build direction two positions were defined, fabricating the samples with the main dimension perpendicular (O1) and parallel (O2) to the building platform (see Figure 1). Finally, the orange surface highlighted in Figure 1 of same samples was remelted using three different parameters configuration (RM1, RM2 and RM3) as described in Table 1. Remelting, in fact, can enhance the surface roughness and the surface relative density [18]. Summarizing the 18 parameter's combination are reported in Table 3.

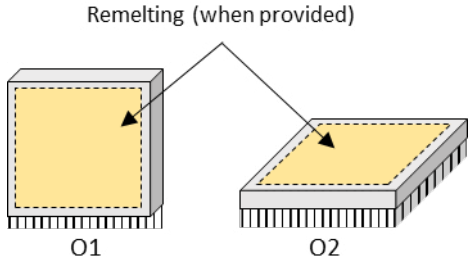


**Fig. 1.** Example of the specimen produced by means of SLM.

Table 3. Parameters set combinations

| **1** | **2** | **3** | **4** | **5** |
|---|---|---|---|---|
| O1+ $MP_1$ | O1+ $MP_2$ | O1+ $MP_3$ | O2+ $MP_1$ | O2+ $MP_2$ |
| **6** | **7** | **8** | **9** | **10** |
| O2+ $MP_3$ | O1+ $MP_1$ + $RM_1$ | O1+ $MP_1$ + $RM_2$ | O1+ $MP_2$ + $RM_1$ | O1+ $MP_2$ + $RM_3$ |
| **11** | **12** | **13** | **14** | **15** |
| O1+ $MP_3$ + $RM_1$ | O1+ $MP_3$ + $RM_3$ | O2+ $MP_1$ + $RM_1$ | O2+ $MP_1$ + $RM_2$ | O2+ $MP_2$ + $RM_1$ |
| **16** | **17** | **18** | | |
| O2+ $MP_2$ + $RM_3$ | O2+ $MP_3$ + $RM_1$ | O2+ $MP_3$ + $RM_3$ | | |

### 2.2 Femto-second peening experiments

The experimental setup for ultrafast laser shock peening is shown in Fig. 2 (a). A Yb:KGW femtosecond laser source (Pharos by Light Conversion) was employed to deliver laser pulses at a wavelength of 1030 nm, duration of 165 fs (full width at half maximum), repetition rate of 6 kilohertz (kHz), and pulse energy of up to 1 mJ. The laser beam was delivered through a laser scan head (intelliSCAN by Scanlab) and a F-Theta objective lens to scan on the sample surface. The surface focal spot size was 34 µm. The aluminum sample was placed on the 3-dimensional motion stage. To study the peening effects, different laser fluences were tested. The laser energy was adjusted by the half-wave plate and beam splitter, then measured by an optical power meter. As shown in Fig. 2 (b), the overlapping ratio, denoted by $\eta$, is to describe and control the distribution of laser pulses on the impact surface, which is expressed as, where D is the spot diameter, Δ is the coincidence length of two successive laser spots, see eq. 1.

$$\eta=\Delta/D^* 100 \quad (1)$$

Table 4 summarizes the processing conditions for the aluminum sample. The laser beam with fluences 44, 88, and 132 J/cm$^2$ of 70% overlapping ratio was introduced to the sample exposed to air.

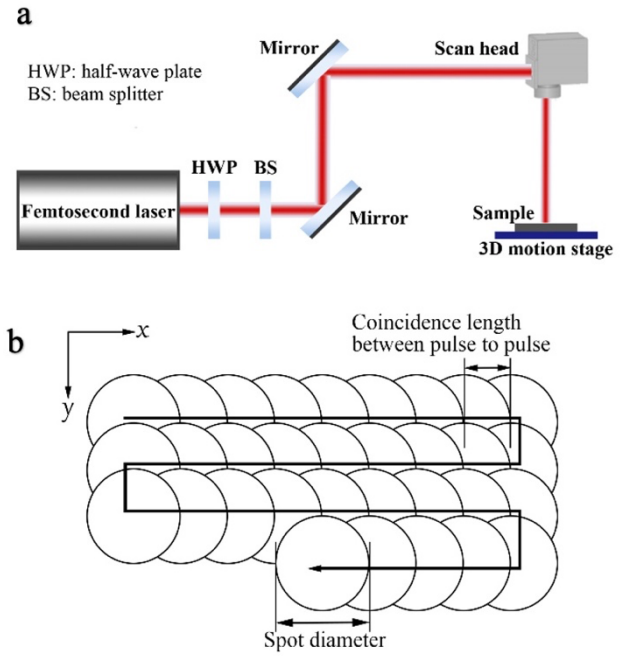


**Fig. 2.** The Schematic illustration of (a) experimental setup, and (b) scan direction of laser pulses for the setup shown in (a).

Table 4. The processing conditions for aluminum sample

| conditions | laser energy (J/cm$^2$) | | |
|---|---|---|---|
| In air | 44 | 88 | 132 |

### 2.3 Sample characterisation

The following attributes of all SLM samples were characterized after peening: microstructure, roughness, and hardness. The roughness was measured with a stylus profilometer in parallel with the building direction, in order to obtain a mean value not affected by the exact direction of the stylus. In fact, it is known that roughness carried out perpendicular to the building direction have high deviation results due to continuous measurement crossings between contiguous layers.

After roughness measurements cross-section of the samples were prepared following standard metallographic procedures and polishing the final surface up to 1 µm. In order to reveal the differences in microstructure due to peening post process, the metallurgical specimens were etched with Keller's reagent with an etching time of 4 s. The microstructure was analyzed by optical microscopy (OM, Nikon Optiphot-100). Finally, Vickers microhardness tests were performed using a durometer with 0.2 kg load (HV0.2) and dwell time of 10 s. Indentations were carried out from the surface to the sample's core with a space between each indentation varying from 70-100 µm.

## 3. Results and discussion

SLM parameters used in this work gave density >99% and a typical microstructure of the as built sample is presented in Fig. 3. In this figure an example of the Vickers measures is also reported. The 2 different microstructures, in the bulk and below the outer surface, are due to the scanning strategy and process parameters used (skin and core). Furthermore, roughness measurements carried out on samples after SLM fabrication show Ra>15 µm for not finished surfaces and Ra of 1.2µm for surfaces milled after SLM. First interesting results obtained was that no laser peening effects were found in rough surfaces: it seems that with Ra>15 µm laser radiation has not been absorbed from the sample and further investigation will be carried out to investigate the importance of the surface roughness on fs-LSP. More in detail, all the samples with vertical build direction have surfaces roughness very close to, or greater than, 10 µm, and so the data obtained are not sufficiently reliable and will not be reported. The upper surface of the horizontally printed samples, on the other hand, has a very high roughness (always larger than 15 µm), but the lower surface, which is directly in contact with the supports and has been milled, has a controlled roughness of 1.2 µm. As a result, the fs-LSP results described below only apply to these surfaces for the sake of consistency.

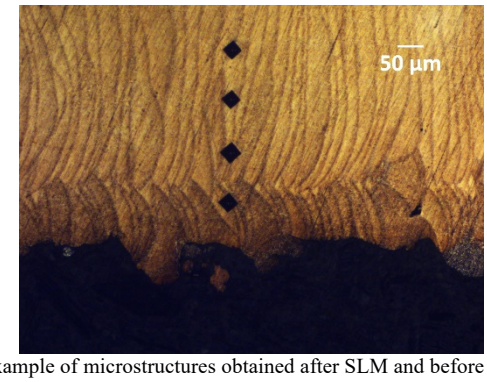


**Fig. 3.** Example of microstructures obtained after SLM and before fs-LSP

Figures 4 and 5 present an example of a metallographic section after fs-LSP obtained with 2 different process parameters: the highest fluence (132 J/cm$^2$) and the lowest fluence (44 J/cm$^2$), respectively. In all samples, there are clearly visible 3 different zones:

- a resolidified area (below the surface)
- a zone with a refined grain
- bulk material

The resolidified zones are caused by the presence of a substrate that is melted during the interaction with the fs-laser and then resolidifies when the samples are cooled in air. Its width is determined by the amount of energy delivered to the sample, which is determined by the laser's energy per pulse and scanning speed (laser energy), and the scanning strategy. The presence of a solidification area was seen in all the settings tested in this study. These areas, in addition to having a high porosity, also have a low hardness and must be reduced or deleted by means of a process optimization campaign.

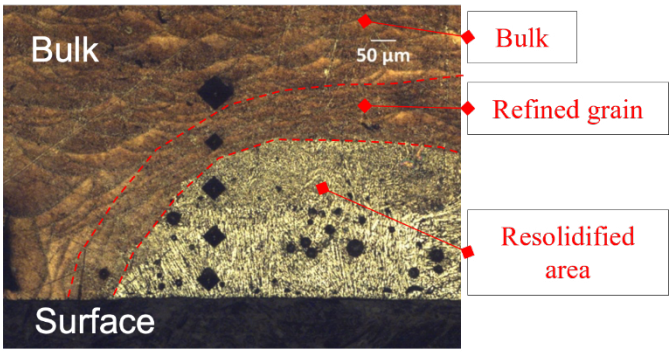


**Fig. 4.** Optical micrograph obtained with 352 J/cm$^2$ fs-LSP

More research will be done in the future to try to figure out the best process parameters to reduce the melted regions, considering the aluminum's low absorption at 1030 nm wavelength and its strong thermal conductivity. Refined grain zones are always below the melted zones, and they are characterized by higher hardness compared to the melted zone and the base material. Table 5 reports the hardness measurements of micrographs in figures 4 and 6, respectively. It is confirmed that zones with refined grain, below the melted area, have the highest hardness, higher than the hardness of the base material of 117 HV (Ref lines in figures).

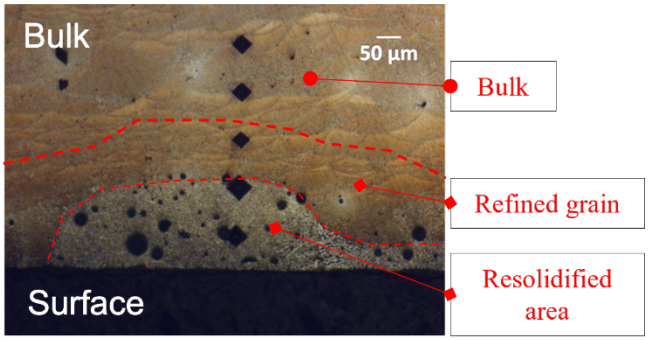


**Fig. 6.** Optical micrograph obtained with 88 J/cm$^2$ fs-LSP

Table 5. Vickers hardness of samples with 352 J/cm$^2$ and 88 J/cm$^2$ fs-LSP.

| REF value 117 HV | | | |
|---|---|---|---|
| Sample with 352 J/cm² | | Sample with 88 J/cm² | |
| Distance from the surface [µm] | Vickers hardness [HV] | Distance from the surface [µm] | Vickers hardness [HV] |
| 35 | 80 | 60 | 80 |
| 130 | 96 | 140 | 65 |
| 210 | 80 | 240 | 140 |
| 350 | 143 | 320 | 118 |
| 390 | 118 | 410 | 115 |

Our preliminary experiments also confirmed that as the laser fluences are raised, the extension of the resolidified area increases, although there are no clear correlations between the extent of the refined grain zone and the hardness with laser fluences.

## 4. Conclusions

The results of a first experimental campaign aiming at determining the effect of a fs laser peening treatment on the substrate of AlSi10 samples produced by SLM are presented in this work. The SLM samples were printed with optimum parameters (density > 99%) in both vertical and horizontal printing directions. To achieve three distinct fluences, the peening treatment was carried out by varying the energy per pulse, scanning speed, and shot overlap. The study showed that:

1. Surface roughness must be reduced when utilizing a fs-laser.
2. A hardness re-solidification area and a fine grain area with a hardness greater than the material's bulk hardness are obtained on the samples where the peening process took place.

In future works, the influence of the surface roughness on the laser absorption will be studied. Afterwards, the peening process will be optimized, trying to reduce the reflow zones and the residual stresses induced by the process will be measured.

## References

[1] M.-Z. Ge, J.-Y. Xiang. "Effect of laser shock peening on microstructure and fatigue crack growth rate of AZ31B magnesium alloy". *J Alloy Compd*, 680 (2016), pp. 544-552, 10.1016/j.jallcom.2016.04.179

[2]M. Tsuyama, Y. Kodama, Y. Miyamoto, I. Kitawaki, M. Tsukamoto, H. N akano. "Effects of Laser Peening Parameters on Plastic Deformation in Stainless Steel". *J Laser Micro Nanoen,* 11 (2) (2016), pp. 227-231, 10.2961/jlmn.2016.02.0013

[3]H. Nakano, M. Tsuyama, S. Miyauti, T. Shibayanagi, M. Tsukamoto. "Femtosecond and Nanosecond Laser Peening of Stainless Steel". J Laser Micro Nanoen, 5 (2) (2010), pp. 175-178, 10.2961/jlmn.2010.02.0014.

[4] A.K. Gujba, M. Medraj. "Laser peening process and its impact on materials properties in comparison with shot peening and ultrasonic impact peening". *Materials* (Basel), 7 (12) (2014), pp. 7925-7974, 10.3390/ma7127925.

[5] G. Tani, L.Orazi, A. Fortunato, A. Ascari, G. Campana "Warm Laser Shock Peeing: New Developments and Process Optimizatio," *CIRP Annals Vol.* 60, pp. 219-222, 2011, doi: 10.1016/j.cirp.2011.03.115.

[6] Sano T, Eimura T, Kashiwabara R, Matsuda T, Isshiki Y, Hirose A. "Femtosecond laser peening of 2024 aluminum alloy without a sacrificial overlay under atmospheric conditions". *Journal of Laser Applications*. 2017. 29, 012005. doi.org/10.2351/1.4967013

[7] Nakhoul1 A, Rudenko A, Sedao X, Peillon N, Colombier J P, Maurice C, Blanc G, Borbély A, Faure N, Kermouche1 G." Energy feedthrough and microstructure evolution during direct laser peening of aluminum in femtosecond and picosecond regimes". *Journal of Applied Physics*. 2021. 130: 015104. doi.org/10.1063/5.0052510

[8] O'Keefe JD, Skeen CH, York CM. Laser-induced deformation modes in thinmetal targets. *J Appl Phys* 1973; 44 (10): 4622–6. doi.org/10.1063/1.1662012.

[9] Peyre P, Fabbro R. Laser shock processing: A review of the physics andapplications. *Opt Quant Electron* 1995; 27 (12):1213–29. doi.org/10.1007/BF00326477.

[10] Montross CS, Florea V, Swain MV. The influence of coatings on subsurfacemechanical properties of laser peened 2011–T3 aluminum. *J Mater Sci* 2001; 36(7) :1801–7. doi.org/10.1023/A:1017537011772.

[11] Nguyen TTP, Tanabe R, Ito Y. Influences of Focusing Conditions on Dynamics of Laser Ablation at a Solid–Liquid Interface. *Appl. Phys. Express* 2013; 6(12):122701. doi.org/10.7567/APEX.6.122701.

[12] Nguyen TTP, Tanabe R, Ito Y. "Laser-induced shock process in under-liquidregime studied by time-resolved photoelasticity imaging technique". *Appl.Phys. Lett.* 2013;102(12):124103.https://doi.org/10.1063/1.4798532.

[13] Le Harzic R, Huot N, Audouard E, Jonin C, Laporte P, Valette S, Fraczkiewicz A,Fortunier R. Comparison of heat-affected zones due to nanosecond andfemtosecond laser pulses using transmission electronic microscopy. *Appl.Phys. Lett.* 2002; 80 (21): 3886–8. doi.org/10.1063/1.1481195.

[14] Nakano H, Miyauti S, Butani N, Shibayanagi T, Tsukamoto M, Abe N.Femtosecond Laser Peening of Stainless Steel. *J Laser Micro Nanoen* 2009; 4(1) :35–8 doi.org/10.2961/jlmn.2009.01.0007.

[15] Li Y, Ren Z, Jia X, Yang W, Nassreddin N, Dong Y, Ye C, Fortunato A, Zhao, X. "The Effect of the Confining Medium and Protective Layer during Femtosecond Laser Shock Peening", *Manufacturing Letters*. 2021, (27), 26-30. doi.org/10.1016/j.mfglet.2020.11.006

[16] Tonelli L, Liverani E, Valli G, Fortunato A, Ceschini L, "Effects of powders and process parameters on density and hardness of A357 aluminum alloy fabricated by selective laser melting", *The international Journal of Advanced Manufacturing Technology.* 2020, 106, 371-383. doi.org/10.1007/s00170-019-04641-x

[17]Tradowsky U, White J, Ward R M, Read N, Attallah M M, Reimers W, "Selective laser melting of AlSi10Mg: Influence of post-processing on the microstructural and tensile properties development", *Materials & Design*. 2016. 105, 212-222. doi.org/10.1016/j.matdes.2016.05.066

[18] Bin L, Bao Qiang L, Zhonghua L, "Selective laser remelting of an additive layer manufacturing process on AlSi10Mg", *Results in Physics*, 2019, 12 982-988. doi.org/10.1016/j.rinp.2018.12.018